JOURNAL OF
BUILDING
PHYSICS

Journal of Building Physics
34(4) 325–350

DOI: 10.1177/1744259110388266
jen.sagepub.com
SAGE

Numerical simulation of heat transfer through hollow bricks in the vertical direction

Zbynek Svoboda and Marek Kubr

Abstract

This article focuses on the numerical modeling of the heat transfer in vertical cavities with small cross-sectional areas in hollow bricks heated from below by means of the computational fluid dynamics (CFD) analysis. The major aim is to specify the ratios between the equivalent thermal conductivities in vertical and horizontal directions ($\lambda_{eq,v}/\lambda_{eq,h}$) for various types of hollow brick masonry. These ratios are not given by brick producers, though they are very important when assessing certain types of thermal bridges. This article presents the governing equations for CFD analysis, together with the main assumptions and boundary conditions. The validation of the FLOVENT CFD commercial code is also discussed, as are the effects of calculation mesh refinement. The results of the first analysis – vertical heat transfer in a single high cavity – show a strong influence of the cross-sectional area of the cavity on the natural convection. While the convective heat transfer for the heat flow in the downward direction is negligible for all considered cross-sectional areas, the natural upward convection disappears only for very high and narrow cavities. Such effects can also be seen in the results of the calculation of the ratio between the equivalent thermal conductivities in the vertical and horizontal directions for the model masonry or for actually produced hollow brick masonry. This ratio is smaller than 1.0 for downward heat flow and between 1.0 and 1.5 for upward heat flow in bricks with a small number of large cavities. By contrast, bricks with a large number of small cavities show almost the same ratio for both vertical directions of heat flow (from 2.2 to 2.7 depending on the actual honeycomb structure).

Faculty of Civil Engineering, Czech Technical University in Prague, Thakurova 7, 166 29 Prague, Czech Republic.

Corresponding author:
Zbynek Svoboda, Faculty of Civil Engineering, Czech Technical University in Prague, Thakurova 7, 166 29 Prague, Czech Republic
Email: svobodaz@fsv.cvut.cz

Keywords
hollow bricks, heat transfer, natural convection, equivalent thermal conductivity, computational fluid dynamics, numerical analysis

Date received: 27 July 2010

Introduction

Hollow bricks with vertically oriented cavities are widely used in the present-day building industry in order to reduce heat transfer through walls. In general, hollow bricks are masonry units with a ratio of less than 0.75 between the net cross-sectional area (solid area) and the total cross-sectional area. The smaller this ratio, the lower the heat transfer through the masonry usually is. The most sophisticated present-day hollow bricks are designed to have equivalent thermal conductivity (including the effects of thermal joints at mortar beds) less than 0.1 W/(m-K). This level can be achieved using a lightweight ceramic body with a honeycomb structure with a large number of small vertical cavities (Figure 1), together with advanced systems of bricklaying (e.g., special mortar applied with a roller 1 mm in thickness).

Due to the prevailing direction of the heat flow through walls, brick producers concentrate on specifying the equivalent thermal conductivity of masonry in the horizontal direction (either by means of measurement or by means of numerical simulations). The equivalent thermal conductivity of masonry for heat flow in the vertical direction is mostly unknown. This is not a problem in most common cases, for example, in the case of calculating the thermal transmittance of a wall or in the case of hygro-thermal evaluation of some typical thermal bridges, such as wall corners. Nevertheless, the equivalent thermal conductivity of masonry in the vertical direction is of high importance in the case of specific two-dimensional or three-dimensional thermal bridges, where a considerable vertical heat flow appears (Figure 2). For such thermal bridges, a calculation of the internal surface temperature factor and linear or point thermal transmittances according to EN ISO 10211 (2007) can show significant errors if the equivalent thermal conductivity of the masonry is taken as being the same in all directions. Since the hollow brick structure is optimized for horizontal heat flow, the vertical heat transfer through the masonry can be considerably higher. The difference between the horizontal and vertical heat flows is caused mainly by continuous honeycomb walls in the vertical direction, but the air convection in larger cavities can also have a noticeable effect.

Generally speaking, heat transfer through hollow bricks involves conduction in all domains and natural convection and radiation in the air cavities. Many researchers have focused on this problem in recent decades, either from the point of view of the numerical accuracy of the calculation, or from the point of view of potential improvements to hollow bricks, for example, Vasile et al. (1998), Al-Hazmy (2006), Laccarrière et al. (2003), Lorente et al. (1996), Branco et al.

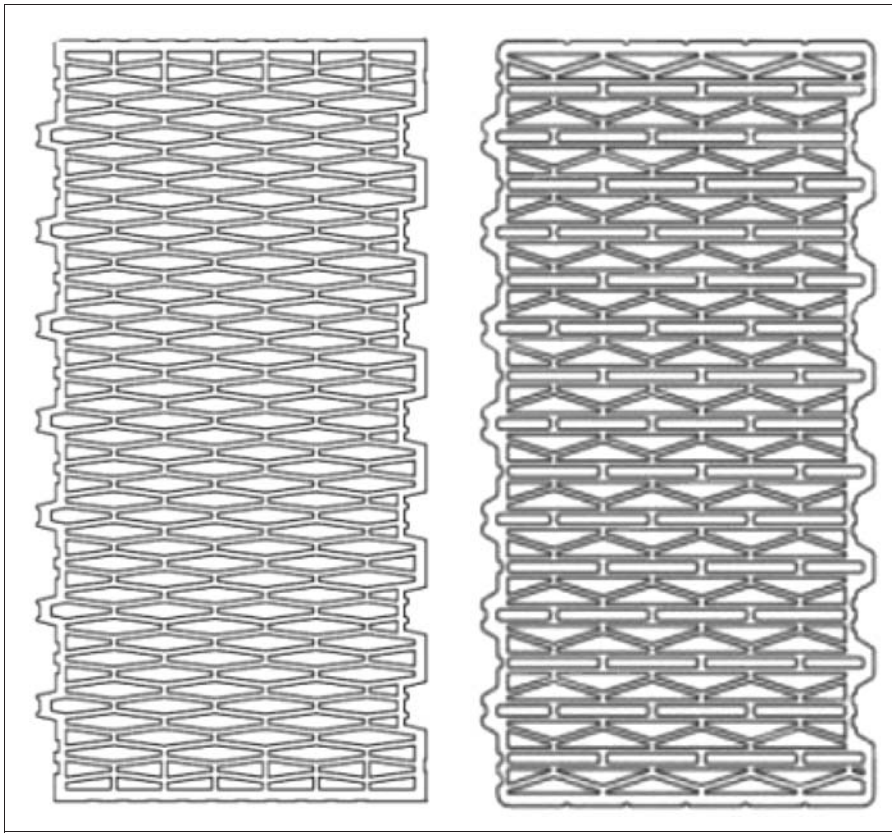

Figure 1. Examples of the typical honeycomb structure of advanced hollow bricks.

(2004), dos Santos and Mendes (2009), del Coz Díaz et al. (2008), and Boukendil et al. (2009). A very comprehensive overview of the state-of-the-art in this field was recently presented by Sun and Fang (2009). Most analyses deal with a typical two-dimensional arrangement, as shown in Figure 3: an air cavity with one hot ($x = 0$) and one cold envelope wall ($x = W$) and two adiabatic envelope walls ($y = 0$ and $y = H$). Some studies have also aimed to show the influence of heat conduction through the horizontal walls of the cavity (Fusegi and Hyun, 1991; Sun and Fang, 2009), and the results of several three-dimensional analyses have also been published recently (Wakashima and Saitoh, 2004; Li et al., 2008a, b; Sun and Fang, 2009). However, the horizontal direction of heat flow is a common assumption in most studies.

Certain exceptions are nevertheless to be found. The effects of heat flow in the vertical direction in air cavities are discussed for example, in studies by Ait-Taleb et al. (2008), Hasnaoui et al. (1992), Sidik (2009), Corcione (2003), or Calcagni et al. (2005), but mostly with the focus on cavities partly heated from below and

cooled from the sides or from above (with the exception of the study by Ait-Taleb et al. (2008), which also shows the results for downward heat flow). The analyses presented by Ait-Taleb et al. (2008), Hasnaoui et al. (1992), Sidik (2009), Corcione (2003), and Calcagni et al. (2005) are also limited to two-dimensional cases, assuming rather small vertical dimensions of the cavities (the aspect ratio between the height and the width of the cavity is typically considered to be in the range from

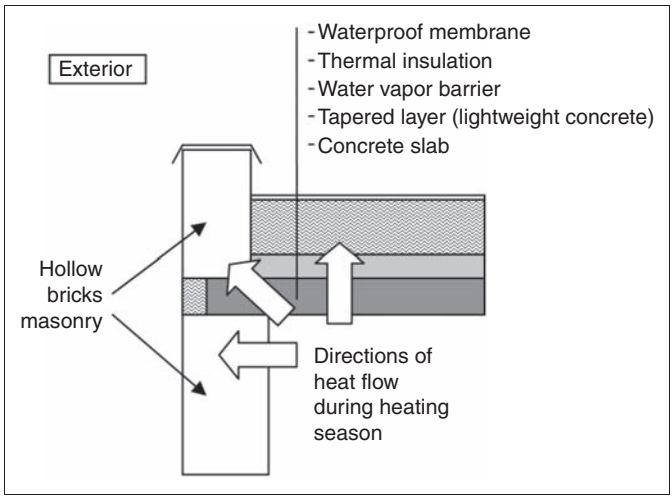

Figure 2. Typical example of a thermal bridge with a considerable vertical heat flow (wall–roof connection).

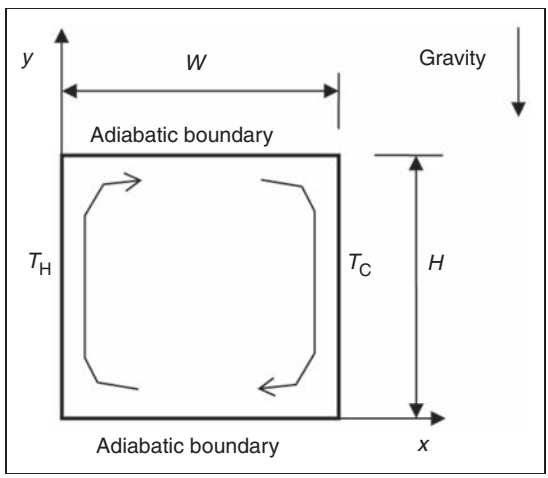

Figure 3. A two-dimensional cavity with two isothermal and two adiabatic walls frequently used for analyses of natural convection.

0.125 to 1). However, the characteristic shapes of the air cavities in honeycomb hollow bricks are completely different: the aspect ratios (height/width) are typically within the range from 1.5 to 25, and hence the results for smaller aspect ratios cannot simply be applied.

The aim of this study is to analyze the heat transfer by conduction, convection, and radiation in hollow brick masonry in the vertical direction using computational fluid dynamics (CFD) analysis. This allows an investigation of some important general issues, such as the influence of the horizontal dimensions of high cavities on vertical heat transfer. The equivalent thermal conductivity in the vertical direction of various hollow bricks masonries can also be calculated and compared to the related standard 'horizontal' equivalent thermal conductivity using this approach.

Governing equations and solution method

The governing partial differential equations for the coupled steady-state air flow and heat transfer through hollow brick masonry (Figure 4) expressed in primitive variables are as follows:

1. conduction equation (in air, mortar and in the ceramic body of bricks):

$$\frac{\partial}{\partial x}\left(\lambda\frac{\partial T}{\partial x}\right)+\frac{\partial}{\partial y}\left(\lambda\frac{\partial T}{\partial y}\right)+\frac{\partial}{\partial z}\left(\lambda\frac{\partial T}{\partial z}\right)=0 \tag{1}$$

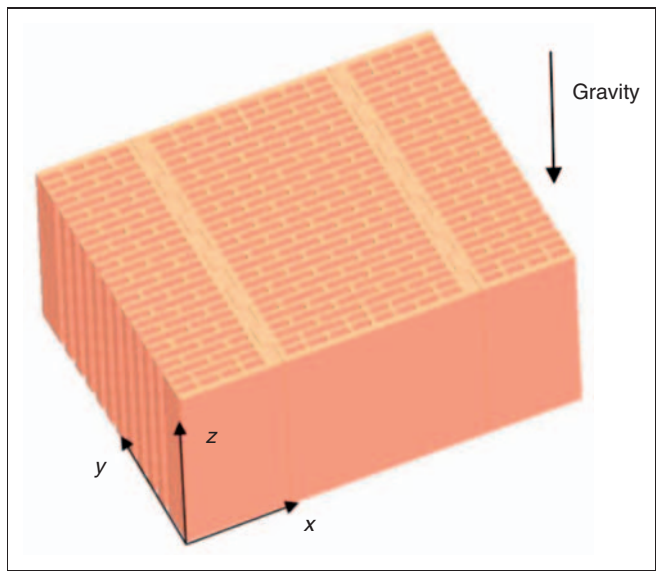

Figure 4. Characteristic segment of hollow brick masonry with coordinate system.

2. continuity equation (in air cavities):

$$\frac{\partial u}{\partial x}+\frac{\partial v}{\partial y}+\frac{\partial w}{\partial z}=0 \tag{2}$$

3. momentum equations in all three directions (in air cavities):

$$u\frac{\partial u}{\partial x}+v\frac{\partial u}{\partial y}+w\frac{\partial u}{\partial z}=-\frac{1}{\rho}\frac{\partial p}{\partial x}+\nu\left(\frac{\partial^2 u}{\partial x^2}+\frac{\partial^2 u}{\partial y^2}+\frac{\partial^2 u}{\partial z^2}\right) \tag{3}$$

$$u\frac{\partial v}{\partial x}+v\frac{\partial v}{\partial y}+w\frac{\partial v}{\partial z}=-\frac{1}{\rho}\frac{\partial p}{\partial y}+\nu\left(\frac{\partial^2 v}{\partial x^2}+\frac{\partial^2 v}{\partial y^2}+\frac{\partial^2 v}{\partial z^2}\right) \tag{4}$$

$$u\frac{\partial w}{\partial x}+v\frac{\partial w}{\partial y}+w\frac{\partial w}{\partial z}=-\frac{1}{\rho}\frac{\partial p}{\partial z}+\nu\left(\frac{\partial^2 w}{\partial x^2}+\frac{\partial^2 w}{\partial y^2}+\frac{\partial^2 w}{\partial z^2}\right)+g\beta(T-T_{\mathrm{r}}) \tag{5}$$

4. energy equation (in air cavities):

$$u\frac{\partial T}{\partial x}+v\frac{\partial T}{\partial y}+w\frac{\partial T}{\partial z}=\frac{\lambda}{\rho_{\mathrm{r}}c}\left(\frac{\partial^2 T}{\partial x^2}+\frac{\partial^2 T}{\partial y^2}+\frac{\partial^2 T}{\partial z^2}\right) \tag{6}$$

with air taken as Newtonian fluid with constant properties except for the density, which is defined using Boussinesq approximation as:

$$\rho=\rho_{\mathrm{r}}[1-\beta(T-T_{\mathrm{r}})]. \tag{7}$$

In the study presented here, the boundary conditions for this set of coupled equations were taken partly as adiabatic without any heat flow over the boundary, and partly as Newton boundary conditions specified as:

$$h(T_{\mathrm{s}}-T_{\mathrm{a}})=-\lambda\frac{\partial T}{\partial n}. \tag{8}$$

The position of the individual boundary conditions on the borders of the solution domain was dependent on the type of analysis (e.g., for the analysis of vertical heat flow, adiabatic conditions were placed at the vertical borders and Newton boundary conditions were placed at the horizontal borders).

Governing Equations (1)–(6) with relevant boundary conditions were solved by means of the finite volume method using commercial FLOVENT CFD software (Mentor Graphics, 2008). The solution algorithm of this software was validated by performing calculations for the benchmark solution of a pure three-dimensional problem: a cubic cavity with two isothermal walls presented by Wakashima and Saitoh (2004). In their study, Wakashima and Saitoh used a cavity filled with air

with an aspect ratio of unity and assumed laminar and incompressible flow (Figure 5). The Prandtl number was taken as 0.71. The benchmark solution was calculated and derived for various Rayleigh numbers and for various uniform calculation grids. In this study, the finest uniform mesh consisting of $120 \times 120 \times 120$ axes was used to calculate the results by means of FLOVENT software and to compare them with the benchmark solution. The results of the comparison are presented in Table 1 using dimensionless velocities expressed (for the x-axis direction) as:

$$u_{\mathrm{dl}} = \frac{u}{U_{\mathrm{r}}} = \frac{u}{\sqrt{g \cdot \beta \cdot H \cdot \Delta T}}. \tag{9}$$

As can be seen, the differences between the benchmark solution taken from Wakashima and Saitoh (2004) and the FLOVENT solution are less than 3% in all cases. The calculated contours of the dimensionless temperature defined as:

$$T_{\mathrm{dl}} = \frac{T - T_{\mathrm{C}}}{T_{\mathrm{H}} - T_{\mathrm{C}}}, \tag{10}$$

which are shown in Figure 6, are also almost identical with the contours presented by Wakashima and Saitoh (2004). They clearly show a strong dependency of the thickness of the vertical boundary layer on the Rayleigh number, and at the same time they also show a noticeable difference between the boundary layers near the vertical and horizontal walls.

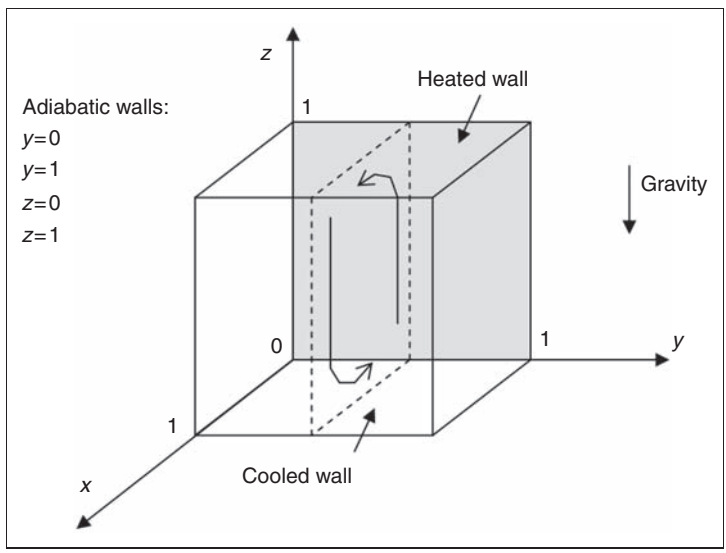

Figure 5. Model cubic cavity with natural convection, according to Wakashima and Saitoh (2004).

Table 1. Comparison between the FLOVENT solution and the benchmark solution for the cubic cavity.

Rayleigh number	Maximum horizontal dimensionless velocity in the *x*-direction on the central line of the cavity ($x = 0.5$, $y = 0.5$)			Maximum vertical dimensionless velocity in the *z*-direction on the central line of the cavity ($y = 0.5$, $y = 0.5$)		
Ra	Benchmark solution	FLOVENT solution	Difference (%)	Benchmark solution	FLOVENT solution	Difference (%)
10^5	0.1416	0.1377	2.75	0.2464	0.2393	2.88
10^6	0.0811	0.0802	1.11	0.2583	0.2531	2.01

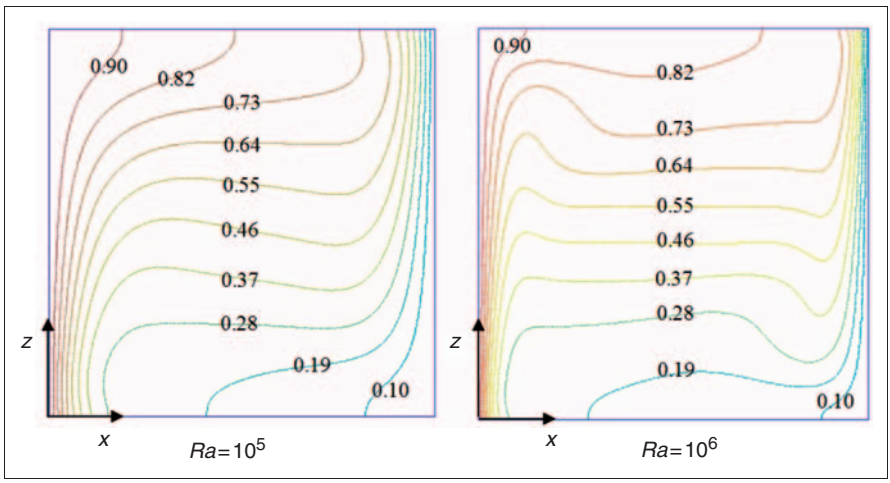

Figure 6. Dimensionless temperature contours in the plane of $y = 0.5$ calculated by means of Equation (10).

All the calculations performed during the validation process used the assumption of laminar flow inside the cavity. The same assumption was also adopted for all the analyses presented further on in this study.

The last mode of heat transfer not yet mentioned – heat transfer by radiation – was calculated in this study by means of the standard high-accuracy radiation model integrated in FLOVENT software. This model uses the following assumptions (Mentor Graphics, 2008):

a. radiative exchange is independent on the frequency of the radiation;
b. radiation is reflected in equal proportions in all directions with no dependency on the angle of incident radiation;

c. effects of both direct and reflected radiations are considered; and
d. no heat is lost from the system except for that which is lost to the exterior environment.

Equivalent thermal conductivity of the masonry

The thermal efficiency of hollow brick masonry is commonly expressed by means of its equivalent thermal conductivity. This physical quantity is a heat-insulating property of the whole wall including hollow bricks, horizontal mortar beds, and vertical joints (either filled with mortar or empty). In order to calculate the equivalent thermal conductivity numerically, it is necessary to create a model of a characteristic segment of the masonry, usually at least one brick with horizontal and vertical joints of half thickness. In the case of modern bricks designed to have empty vertical joints, the characteristic segment must usually have at least two bricks due to the shape of vertical walls of such bricks (Figure 4). Newton boundary conditions (8) are afterwards attached to the appropriate borders of the analyzed characteristic segment and the heat transfer by conduction, convection, and radiation is calculated in order to obtain the total heat flow through the masonry. The equivalent thermal conductivity can subsequently be calculated as:

$$\lambda_{\mathrm{eq}} = \frac{d}{\frac{A \cdot \Delta T}{Q} - \left(\frac{1}{h_{\mathrm{i}}} + \frac{1}{h_{\mathrm{e}}}\right)}, \tag{11}$$

with the heat flow Q derived as the mean value from the heat flows at the internal and external surfaces (results of the calculation by means of FLOVENT software) in order to decrease the simulation deviation. The equivalent thermal conductivity can be calculated using Equation (11) for any direction of the heat flow.

In the analyses presented below, the equivalent thermal conductivity of hollow brick masonry has been derived from the simulation results using the material properties summarized in Table 2.

Mesh generation

Calculating the natural convection in air cavities with various dimensions requires calculation meshes with various grid sizes in order to get accurate CFD simulation results. Larger cavities usually need finer meshes than smaller cavities due to the greater influence of natural convection. It is common practice to perform tests based on repeated calculation of the convection problem for various numbers of cells in the mesh in order to select a suitable grid size for the desired accuracy of the calculation, for example, Al-Hazmy (2006), Sun and Fang (2009). In this study, hollow bricks with air cavities of many different sizes were calculated, and for each specific arrangement the influence of the grid size on the simulation result was analyzed using the following test procedure. In the first step, the maximum distance

Table 2. Material properties used in the calculations.

Material	Density, ρ (kg/m^3)	Specific heat capacity, c (J/(kg-K))	Thermal conductivity, λ (W/(m-K))	Emissivity, ε
Air	1.23	1007	0.0249	–
Standard ceramic brick body	1600	1000	0.50	0.9
Lightweight ceramic brick body	1300	1000	0.30	0.9
Standard mortar	1600	840	0.87	0.9
Lightweight mortar	500	840	0.20	0.9

between the grid axes was taken as 20 mm and simultaneously the mesh was refined near the walls of all air cavities. In the subsequent steps, the number of cells in the mesh was roughly doubled until the difference in the equivalent thermal conductivities in two subsequent steps was less than 1%.

The test procedure can be explained for the case of a model hollow brick with two air cavities (Figure 7), which was assumed in this calculation to be covered by a mortar layer from the top, from the sides, and from below. It is obvious that real masonry from bricks of this type with large cavities cannot be assembled in this way. However, this was just one of the analyzed cases in the study showing the influence of the mean cross-sectional area of the cavities on the ratio between the equivalent thermal conductivities in the vertical and horizontal directions (see the section 'Numerical simulations and results'). As the cross-sectional area of the air cavities decreases (in the rest of the analyzed cases), the application of mortar to this side of the brick creates fewer problems, and for actually produced modern bricks (Figures 1 and 4) thin-layered mortar applied to horizontal joints is a standard solution.

The equivalent thermal conductivity of the model brick presented in Figure 7 was calculated using various stretched meshes (Figure 8) with maximum distances between the grid axes from 20 mm to 2 mm. The number of cells in the mesh was approximately doubled in each step of the test, reaching a total number of almost 2,386,000 cells for the final calculation case. The effect of the gradual mesh refinement is presented in Figure 9. As can be seen, all results show a small difference from the most exact solution (less than 7%). The last two results differ by less than 1%, and so they represent the desired solution.

Numerical simulations and results

Influence of the cross-sectional area on convective heat transfer in a high vertical cavity

In basic technical calculations, the combined convective–conductive heat transfer inside air cavities or layers is usually expressed by means of

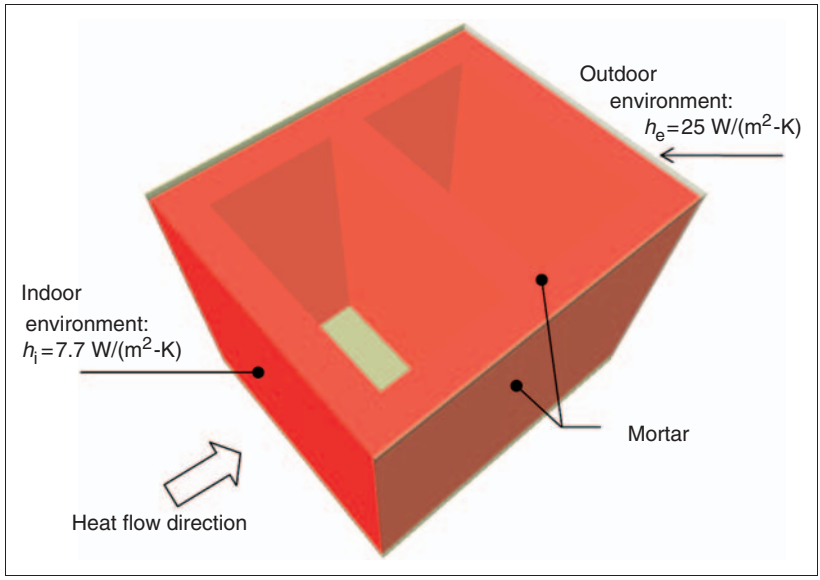

Figure 7. Model hollow brick with two air cavities.

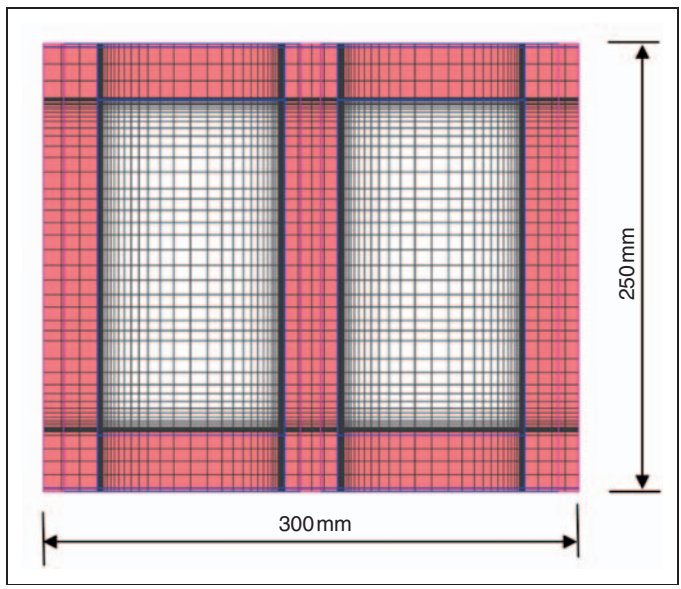

Figure 8. Stretched grid in a horizontal section through the model hollow brick with two cavities.
Note: 10 mm maximum distance between the axes.

a convective/conductive heat transfer coefficient. This quantity is typically used, together with the radiative heat transfer coefficient, as a simple way of determining the equivalent thermal resistance of the air layer, using the formula:

$$R_g = \frac{1}{h_a + h_r}. \tag{12}$$

The convective/conductive heat transfer coefficient h_a is defined in EN ISO 6946 (2007) in dependency on the heat flow direction, the thickness of the air layer in the direction of the heat flow, and on the temperature difference between the cavity walls perpendicular to the heat flow direction. According to EN ISO 6946, the value of h_a is determined by the heat conduction for small air layer thicknesses (approximately up to 12 mm for vertical heat flow) and by natural convection for wider cavities. This technical standard completely neglects the influence of the cross-sectional area of the cavity (i.e., the area in the plane orthogonal to the heat flow direction). It even declares that the convective/conductive heat transfer coefficient is independent from other dimensions apart from the thickness of the air layer.

The aim of the first analysis presented in this study is to find out the actual dependency of the convective/conductive heat transfer coefficient on the dimensions of the air cavity. The height of the analyzed airspace is taken in all cases as 238 mm, since this is the typical height of present-day hollow bricks. The cross-sectional area is considered in the range from 100 cm^2 to 0.25 cm^2 in order to model typical cavity sizes in hollow bricks. The orientation of the heat flow is introduced into the simulation model in two ways: first, from the bottom to the top

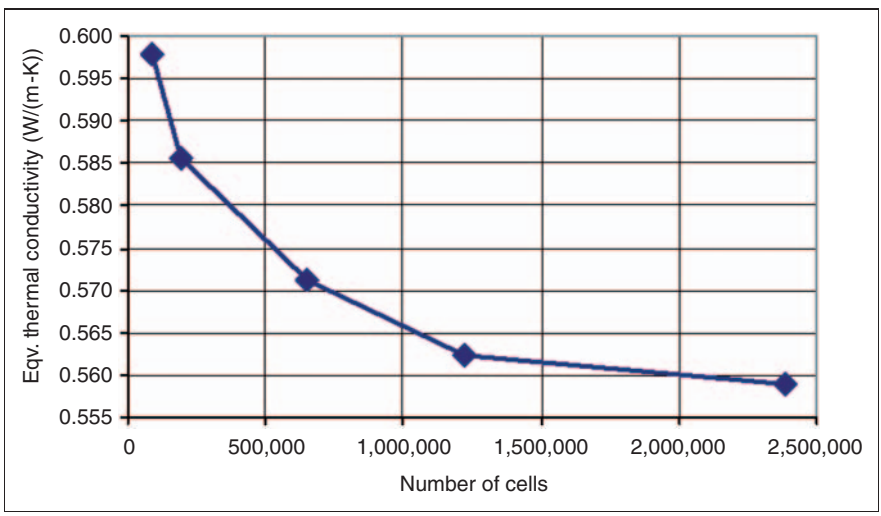

Figure 9. Effect of mesh refinement.

(supporting natural convection) and second, in the opposite direction to verify the negligible convection in such a situation. The temperature difference is taken as 10 K, and the vertical walls of the cavity are assumed to be non-conducting.

Table 3 and Figure 10 show that the calculated heat transfer coefficient h_a is strongly dependent on the horizontal dimensions of the air cavity. This relation is

Table 3. Convective/conductive heat transfer coefficient for the vertical heat flow direction.

Height of the cavity, H (cm)	Cross-sectional area of the cavity, A_c (cm^2)	Rayleigh number, Ra	Convective/conductive heat transfer coefficient, h_a (W/(m^2-K))			
			Heat flow upward		Heat flow downward	
			EN ISO 6946	CFD calculation	EN ISO 6946	CFD calculation
23.80	100.00	1.3×10^6	2.46	2.13	0.26	0.11
	25.00	1.6×10^5		1.63		0.11
	6.25	1.9×10^4		0.84		0.11
	1.00	1.3×10^3		0.11		0.11
	0.25	1.6×10^2		0.11		0.11

The characteristic length used in deriving the Rayleigh number is in this case specified in the same way as for the flow in pipes with a non-circular cross-section, that is, as $4A_c/P$, where A_c is the cross-sectional area of the cavity (m^2) and P its perimeter (m).

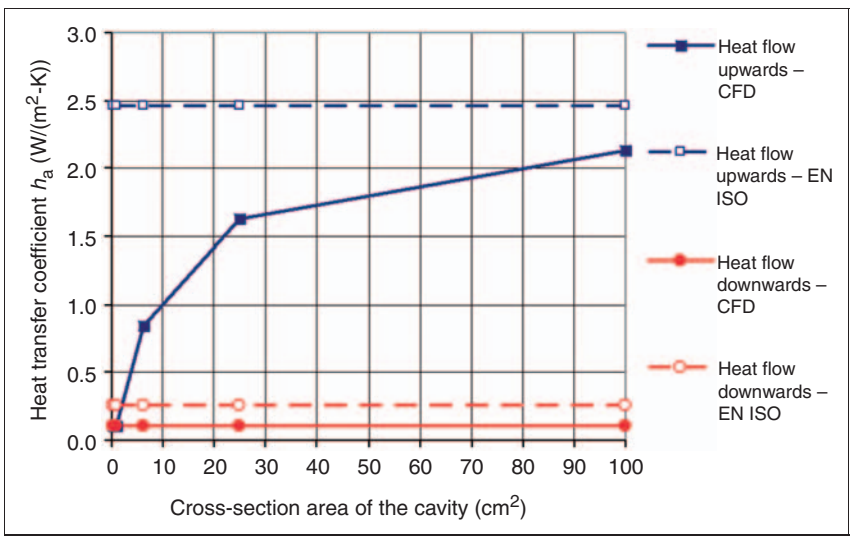

Figure 10. Convective/conductive heat transfer coefficient in a vertical air cavity with variable cross-sectional area.

quite in conflict with the assumption of EN ISO 6946 (2007). It is also worth noting that the values of heat transfer coefficient h_a taken from EN ISO 6946 are in all test cases higher than the values calculated by means of CFD analysis, which means that this standard slightly (and in some cases considerably) overestimates the heat transfer by convection in the vertical direction in air layers with smaller cross-sectional areas. However, this does not necessarily mean that the approach is wrong, since it usually leads to results with a higher safety margin, for example, when calculating the thermal transmittance of building constructions with unventilated air layers.

Another important result of the analysis presented here is that the influence of natural convection disappears even in the case of an upward heat flow when the cross-sectional area of the cavity approaches or falls below 1 cm^2. This limit is of course valid only for the considered cavity height of 238 mm; it would be different for other cavity heights. If we introduce an aspect ratio between the height of the cavity and its characteristic dimension in the horizontal plane, we obtain the value of 23.8 for our limit situation (characteristic horizontal dimension 10 mm and height 238 mm). An aspect ratio higher than 20 could indicate that the natural convection is negligible in the given cavity; but such a general conclusion obviously needs further verification.

In the case of downward heat flow, the analysis results show that natural convection is actually insignificant for all considered cross-sectional areas and the heat transfer coefficient h_a is influenced solely by heat conduction.

Differences between the temperature distributions in cavities with large and small cross-sectional areas are presented in Figure 11 using three-dimensional iso-surfaces. The strongly convective nature of the heat transfer in the large cavity is evident, as is the temperature distribution typical for conduction in the small cavity. The air flow velocity field in the large cavity is particularly interesting (Figure 12), as it is noticeably symmetrical and shows significant effects of the vertical corners on the development of the air flow field. As can be seen, the air flow in the vertical direction (the z-component of the velocity vector) is oriented to the top of the cavity in all corners and to the bottom of the cavity in its center. The three-dimensional iso-surfaces representing the individual velocities are colored by the pressure distribution (in the range from -0.025 to $+0.029$ Pa).

The maximum air flow velocity determined for the given boundary conditions was found to be 0.1120 m/s for the cavity with a cross-sectional area of 100 cm^2 and 0.0001 m/s for the cavity with a cross-sectional area 100 times smaller.

Ratio between equivalent thermal conductivities in vertical and horizontal directions for model hollow brick masonry

The equivalent thermal conductivity of masonry derived assuming horizontal heat flow is one of the standard properties given by brick producers. As was already discussed in the introduction to this study, the equivalent thermal conductivity in the vertical direction is usually missing, although it is essential in many cases.

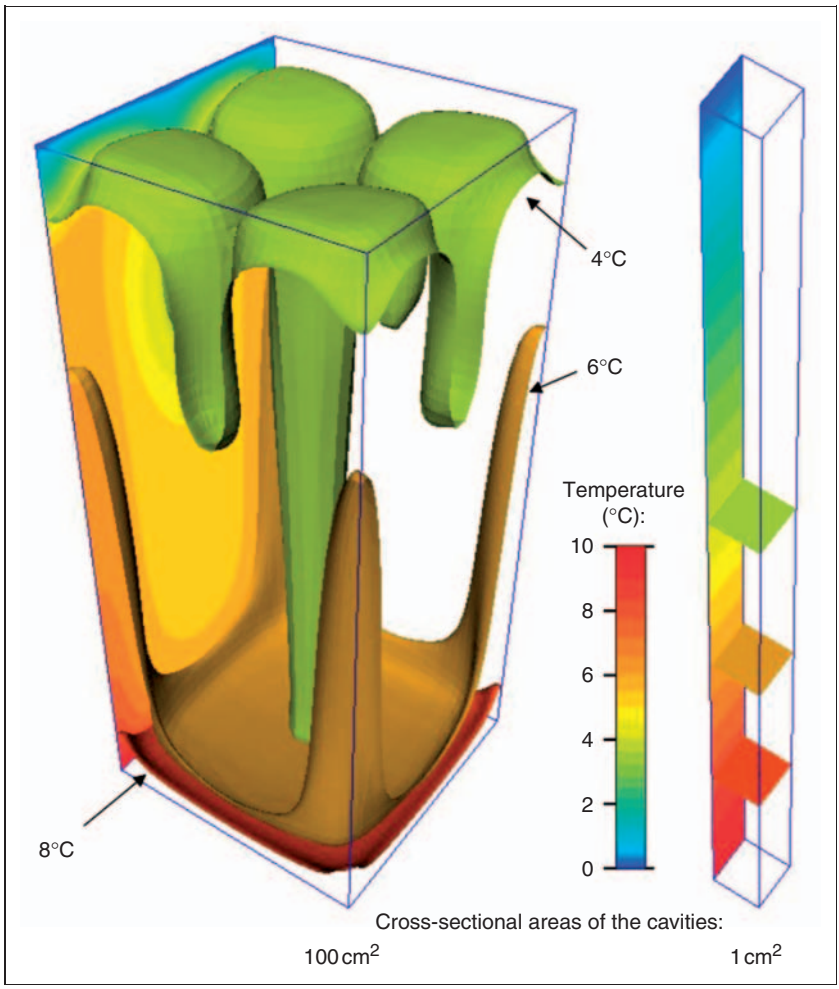

Figure 11. Temperature distribution in vertical cavities with different cross-sectional areas.

A set of model bricks with various numbers of cavities was created, in order to find a general correlation between the two equivalent thermal conductivities. In all cases, the ratio between the net cross-sectional area (the solid area) and the total cross-sectional area was taken as 0.48. This means that the air cavities represent 52% of the total cross-sectional area of the model bricks. This percentage was chosen intentionally because most present-day honeycomb hollow bricks (like the typical examples in Figure 1) have the ratio between the cross-sectional area of the cavities and the total cross-sectional area within the range from 50% to 55%. All bricks were modeled in the CFD analysis as a part of the masonry, that is, with mortar layers from the top, from the bottom, and from the sides (see also the Section 'Mesh generation' with Figure 7). The dimensions of all bricks were

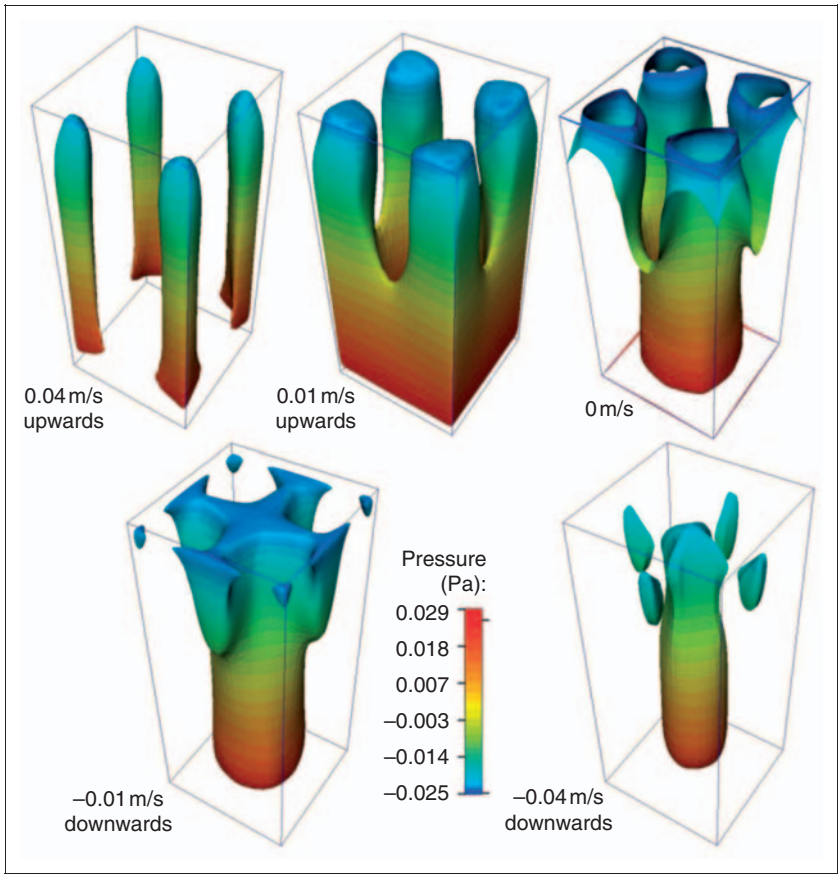

Figure 12. Distribution of the air flow velocity component in the vertical direction in a cavity with a cross-sectional area of 100 cm^2.

chosen as $300 \times 238 \times 247$ mm, with the value of 300 mm being the thickness in the horizontal heat flow direction and the value of 238 mm being the height of the brick. The horizontal mortar layers were considered to be 12 mm in thickness and the vertical mortar joints 3 mm in width. The material properties were taken from Table 2 (standard ceramic brick body and lightweight mortar).

Table 4 and Figure 13 show the results of the CFD simulation for horizontal heat flow and for both orientations of vertical heat flow. The ratio between the equivalent thermal conductivities in vertical and horizontal directions is also presented.

The results show clearly that the equivalent thermal conductivity of the hollow brick masonry in the vertical direction is strongly dependent on the direction of the heat flow and on the mean cross-sectional area of the cavities. Bricks with a small number of large cavities have only a relatively small ratio $\lambda_{eq,v}/\lambda_{eq,h}$ in the upward

Table 4. Equivalent thermal conductivities of the model hollow brick masonry.

Mean cross-sectional area of cavities in bricks, A_c (cm^2)	Number of cavities in one brick	Equivalent thermal conductivity of the masonry for heat flow direction			Ratio between equivalent thermal conductivities	
		Horizontal, $\lambda_{eq,h}$ (W/(m-K))	Upward, $\lambda_{eq,v,u}$, (W/(m-K))	Downward, $\lambda_{eq,v,d}$ (W/(m-K))	In upward and horizontal directions, $\frac{\lambda_{eq,v,u}}{\lambda_{eq,h}}$	In downward and horizontal directions, $\frac{\lambda_{eq,v,d}}{\lambda_{eq,h}}$
196.4	2	0.559	0.593	0.282	1.06	0.50
130.9	3	0.470	0.600	0.287	1.28	0.61
98.2	4	0.408	0.602	0.289	1.48	0.71
78.6	5	0.351	0.610	0.292	1.74	0.83
32.7	12	0.277	0.616	0.309	2.22	1.12
14.5	27	0.222	0.497	0.324	2.24	1.46
5.0	70	0.164	0.371	0.365	2.26	2.23

The Rayleigh number varies from 1.9×10^4 to 4.8×10^6 for the presented calculation cases. For more information about deriving the Rayleigh number, see the note under Table 3.

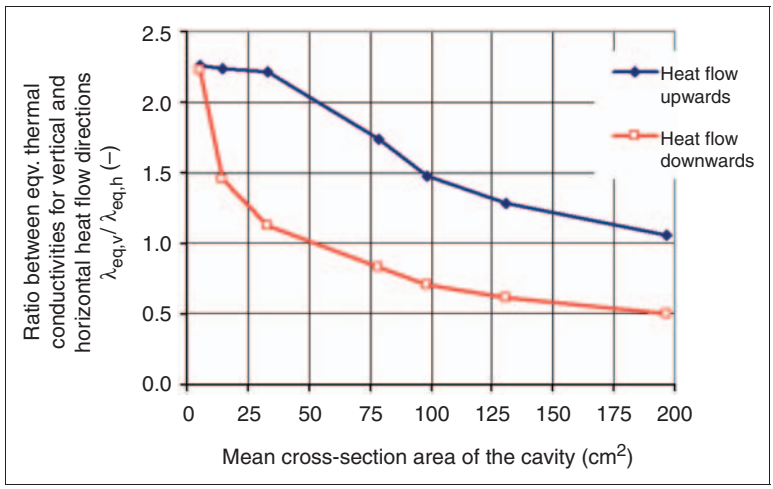

Figure 13. Ratio between the equivalent thermal conductivities of the masonry in vertical and horizontal directions in dependency on the mean cross-sectional area of the cavities in the hollow bricks.

direction (less than 1.5), mainly because their 'horizontal' equivalent thermal conductivity is rather high. At the same time, their ratio $\lambda_{eq,v}/\lambda_{eq,h}$ in the downward direction is less than 1.0, which means that these bricks have even higher thermal resistance in this heat flow direction than in the horizontal direction. Such results

are caused by significant natural convection in the cavities for the horizontal and upward heat flows and by negligible effects of this mode of heat transfer for the downward heat flow. The temperature distribution in the cavities reflects this situation clearly, as shown in Figures 14 and 15 (note especially the difference between the two vertical heat flow directions).

Bricks with a large number of small cavities have completely different ratios between the equivalent thermal conductivities. As the heat transfer by convection in both vertical directions is quite close to or equal to zero, the heat is transferred vertically mainly by conduction. The conductive heat transfer in this direction increases gradually, since there are more and more honeycomb intersections in the cross-section of the brick as the number of cavities rises. The horizontal heat flow is simultaneously limited due to the large number of cavities with small cross-sectional areas. For the case of extremely perforated bricks (Figure 16), the equivalent thermal conductivities of the masonry in the upward and downward

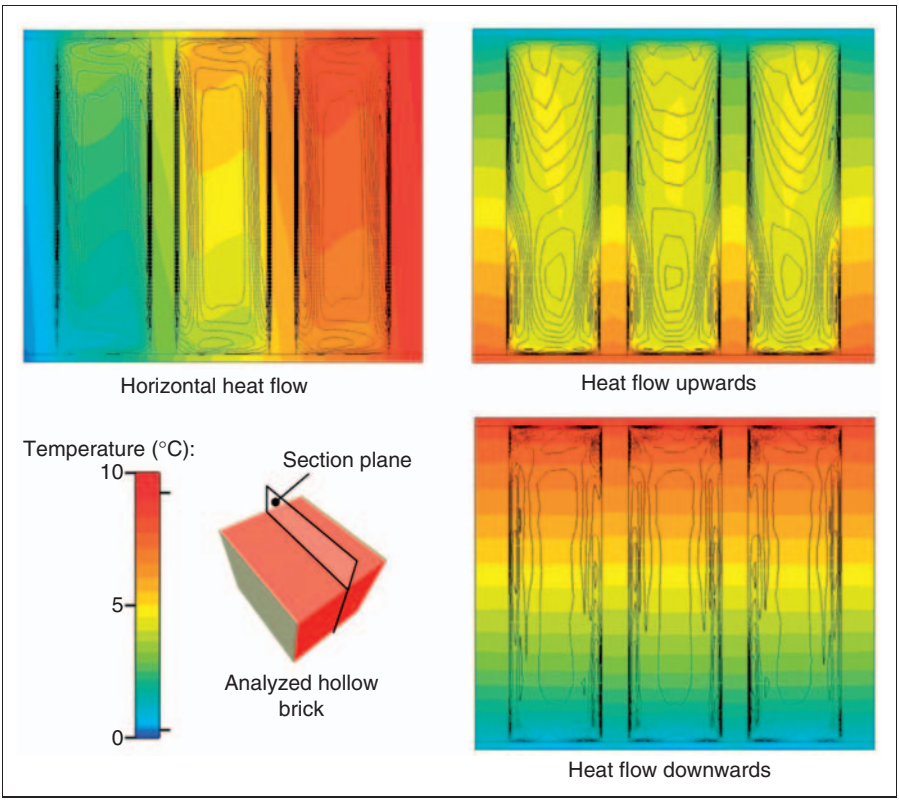

Figure 14. Temperature distribution and air flow velocity contours for various heat flow directions in a brick with three large cavities.

directions are practically the same. The ratio $\lambda_{eq,v}/\lambda_{eq,h}$ for such masonry is stabilized around 2.2, which means that it has more than twice higher equivalent thermal conductivity in the vertical direction than in the horizontal direction. The temperature distributions in the cross-sections through the brick presented in Figures 16 and 17 confirm that heat conduction is the prevailing mode of heat transfer. The deformation of the temperature field by the convection typical for hollow bricks with large cavities (Figure 15) cannot be found in any part of the brick in this case. The temperature iso-surfaces in Figure 17 are colored by the magnitude of the heat flow rate, which also enables the heat flow rate distribution to be shown with clear differences between the ceramic brick body and the cavities.

Vertical heat transfer in actually produced hollow brick masonry

The model hollow bricks discussed in the previous section do not correspond exactly with the actually produced hollow bricks. Although the cross-sectional area of the cavities in the model bricks is basically the same as in the case of the real hollow bricks, the authentic honeycomb structure (Figure 1) is considerably more complicated than the ceramic body structure considered for the model bricks in the previous section (Figure 16). This could lead to deviations from the ratios $\lambda_{eq,v}/\lambda_{eq,h}$ presented for the model brickwork in Table 4.

In order to test the differences between the model masonry and the real brick masonry, three typical hollow bricks with vertical cavities were chosen from the current production range of a present-day brick factory. The brick producer declares the usual 'horizontal' equivalent thermal conductivities for masonries

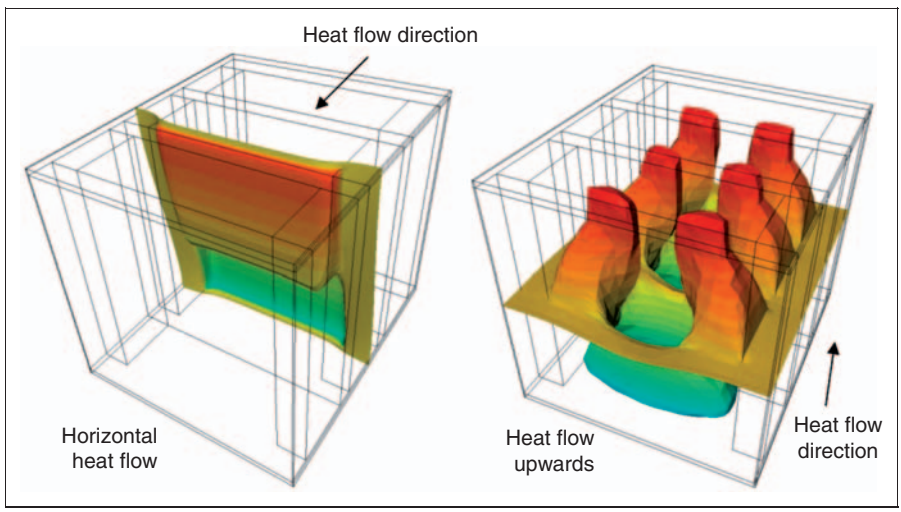

Figure 15. Iso-surfaces representing 4.5°C for the horizontal and upward heat flow directions in a brick with three large cavities.

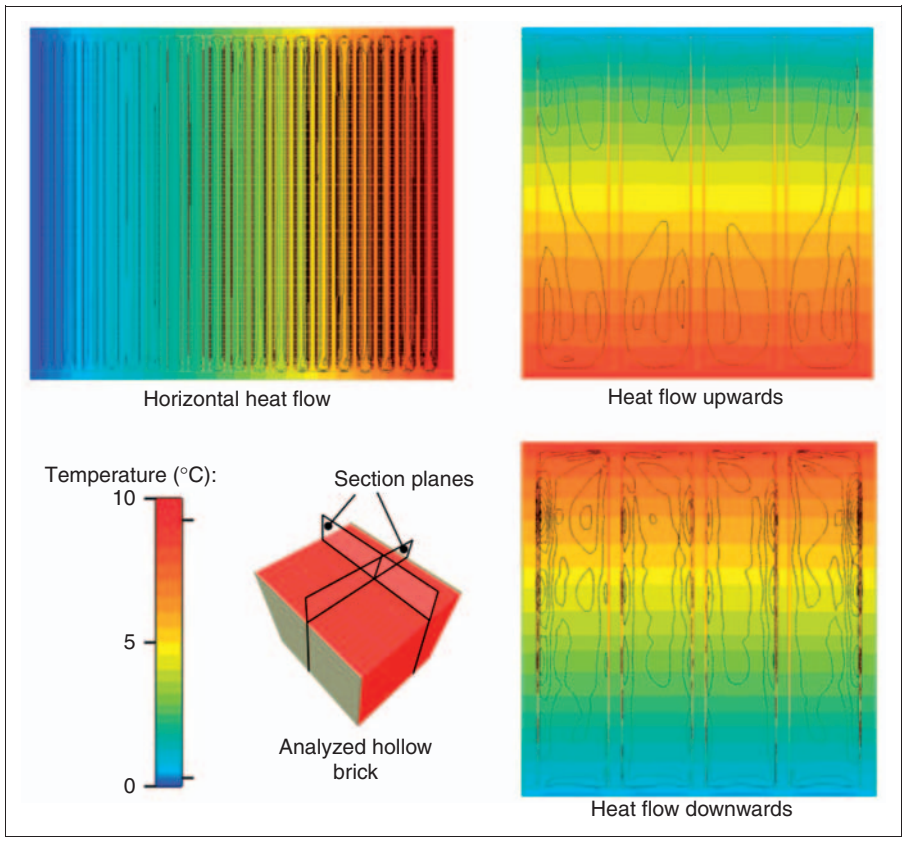

Figure 16. Temperature distribution and air flow velocity contours for various heat flow directions in a brick with 70 small cavities.

from all chosen bricks. These values were obtained either by means of measurements performed on a large segment of masonry (brick 440 mm in thickness) or by means of combined measurement and calculation according to EN 1745 (2002). The second approach was used in the case of bricks 300 and 400 mm in thickness (the thermal conductivity of the brick body was measured, and the equivalent thermal conductivity of the masonry was calculated).

The measurement of the thermal resistance of the brick masonry 440 mm in thickness was carried out using the test procedure in accordance to EN ISO 8990 (1996) in the usual horizontal heat flow direction without internal and external plasters (CSI, 2002). The dimensions of the measured masonry segment were $1700 \times 1750 \times 440$ mm. The equivalent thermal conductivity of the masonry was subsequently calculated from the measured thermal resistance with the following result: $\lambda_{eq,h} = 0.152$ W/(m-K). This value is valid for masonry with lightweight mortar and for an average moisture content of 1%.

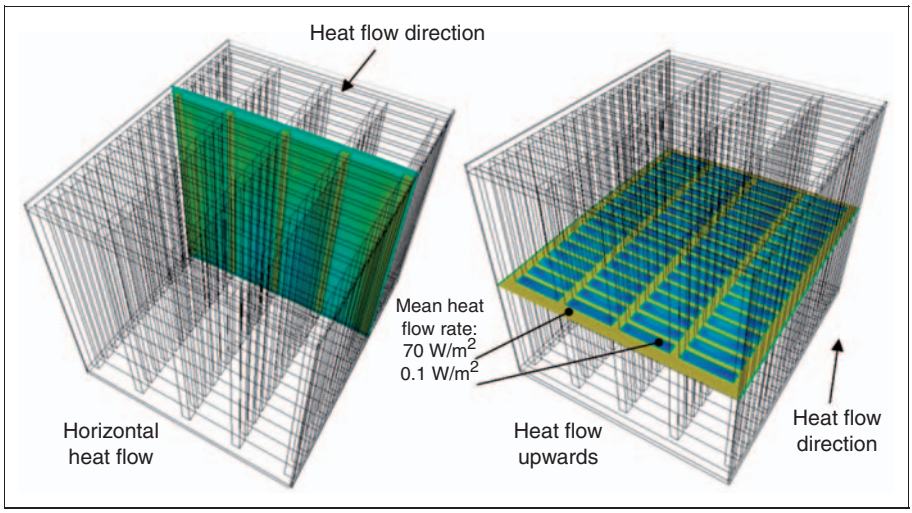

Figure 17. Iso-surfaces representing 4.5°C for horizontal and upward heat flow directions in a brick with 70 small cavities.

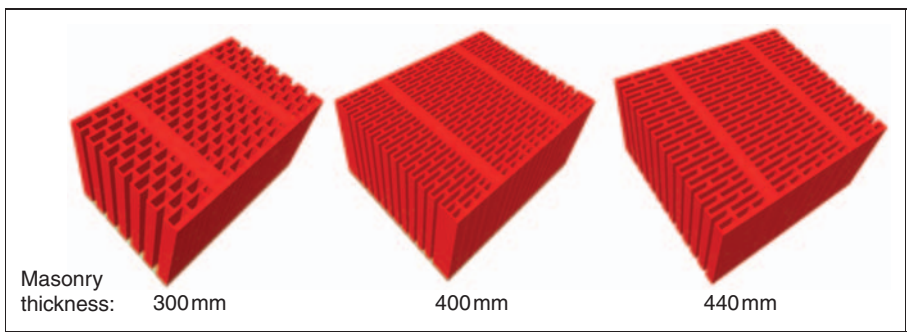

Figure 18. CFD models of characteristic segments of hollow brick masonry.

The measurement results presented here and the declared equivalent thermal conductivities for two other types of the masonries were used for partial verification of the CFD calculation results. The calculation models of all three characteristic masonry segments used in the CFD analysis are shown in Figure 18. The corresponding CFD simulation results are presented in Table 5 and in Figure 19. All results were calculated with the assumption of laminar air flow in the cavities and for the material properties taken from Table 2 (standard ceramic brick body for masonry 300 mm in thickness, lightweight ceramic brick body for masonry 400 and 440 mm in thickness, and lightweight mortar for all cases). As shown in Table 5, the calculated equivalent thermal conductivities for the horizontal direction differ by not more than 3.5% from the partially or completely measured values.

Table 5. Equivalent thermal conductivities of the real hollow brick masonry.

	Equivalent thermal conductivity of the masonry for heat flow direction				Ratio between equivalent thermal conductivities	
	Measurement (partial or complete)	CFD calculation				
Thickness of masonry, d (mm)	Horizontal, $\lambda_{eq,h,test}$ (W/(m-K))	Horizontal, $\lambda_{eq,h,CFD}$ (W/(m-K))	Upward, $\lambda_{eq,v,u,CFD}$ (W/(m-K))	Downward, $\lambda_{eq,v,d,CFD}$ (W/(m-K))	In upward and horizontal directions, $\frac{\lambda_{eq,\,v,\,u}}{\lambda_{eq,\,h}}$	In downward and horizontal directions, $\frac{\lambda_{eq,\,v,\,d}}{\lambda_{eq,\,h}}$
300	0.250	0.259	0.565	0.561	2.18	2.17
400	0.131	0.132	0.353	0.350	2.67	2.65
440	0.152	0.156	0.380	0.377	2.44	2.42

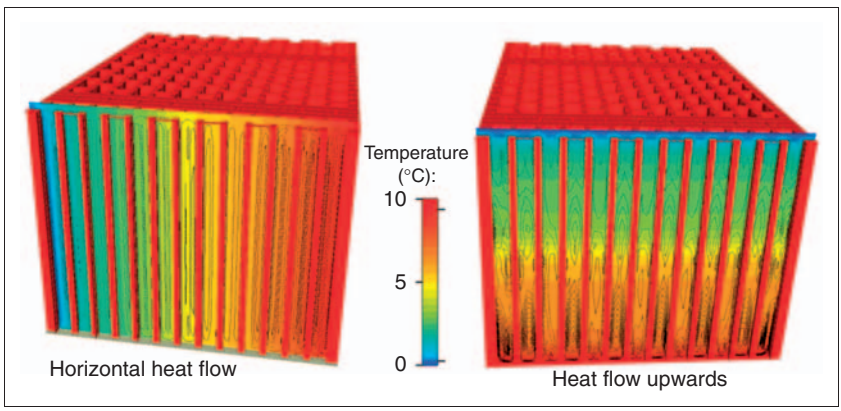

Figure 19. Temperature distribution and air flow velocity contours in masonry 300 mm in thickness.

The ratio between the equivalent thermal conductivities in vertical and horizontal directions varies from 2.2 to 2.7 in dependency on the type of bricks. The correlation of this ratio to the ratio given for the model bricks in Table 4 is excellent for masonry 300 mm in thickness. In the cases of masonry 400 and 440 mm in thickness, there are certain differences probably because the real brickwork has a more sophisticated structure than the model brickwork and has lower equivalent thermal conductivity in the horizontal direction. It is possible that in the case of even more advanced bricks (Figure 1), the ratio $\lambda_{eq,v}/\lambda_{eq,h}$ would also be higher than 2.2. This problem will form the focus of future research.

Conclusion

The heat transfer in the vertical direction in hollow brick masonry has been studied by means of CFD analysis for a single vertical cavity and also for various models and actually produced bricks. The main results of the numerical simulations can be summarized as follows:

1. natural convection in a vertical cavity heated from below is strongly influenced by its cross-sectional area;
2. convective heat transfer in the cavity in vertical direction disappears almost completely when the height of the cavity is more than 20 times greater than the characteristic dimension of the cavity in the horizontal plane. In such cavities, conduction and radiation are the only modes of heat transfer;
3. heat transfer by natural convection for the downward heat flow direction is negligible for all considered cross-sectional areas of the cavities;
4. the ratio between the equivalent thermal conductivities of hollow brick masonry in vertical and horizontal directions ($\lambda_{eq,v}/\lambda_{eq,h}$) depends on the mean cross-sectional area of the cavities in the bricks and on the direction of the heat flow;
5. brick masonry with a small number of large cavities has this ratio smaller than 1.0 for downward heat flow and within the range from 1.0 to 1.5 for upward heat flow; and
6. this ratio is almost the same for both vertical directions of heat flow for brick masonry with a large number of small cavities, since the convective heat transfer is minimized due to the small cross-sectional areas of the cavities in the bricks; the actual values of the ratio $\lambda_{eq,v}/\lambda_{eq,h}$ depend on the arrangement of the honeycomb structure in the cross-section of the brick, and vary from 2.2 to 2.7 according to the simulation results presented here.

This study has focused on model brick masonry and on actually produced but simpler hollow brick masonry. Further research is therefore planned in order to specify the ratios $\lambda_{eq,v}/\lambda_{eq,h}$ also for other types of more complicated honeycomb hollow brick masonry.

Nomenclature

A = Area of the characteristic segment of the masonry perpendicular to the heat flow direction (m^2)
A_c = Cross-sectional area of a cavity (m^2)
c = Specific heat (J/(kg-K))
d = Thickness of the masonry (m)
g = Gravitational acceleration (m/s^2)
h = Surface heat transfer coefficient ($W/(m^2\text{-}K)$)
h_a = Conductive/convective heat transfer coefficient ($W/(m^2\text{-}K)$)
h_i = Internal surface heat transfer coefficient ($W/(m^2\text{-}K)$)

h_e = External surface heat transfer coefficient (W/(m^2-K))
h_r = Radiative heat transfer coefficient (W/(m^2-K))
H = Height of the cavity (m)
p = Pressure (Pa)
Q = Heat flow (W)
Ra = Rayleigh number
R_g = Thermal resistance of an airspace (m^2 K/W)
T = Temperature (K)
T_a = Ambient temperature (K)
T_C = Temperature at the cold surface (K)
T_{dl} = Dimensionless temperature
T_H = Temperature at the hot surface (K)
T_r = Reference temperature (K)
T_s = Surface temperature (K)
u = Velocity component in the x-axis direction (m/s)
u_{dl} = Dimensionless velocity component in the x-axis direction
U_r = Reference velocity (m/s)
v = Velocity component in the y-axis direction (m/s)
w = Velocity component in the z-axis direction (m/s)
W = Width of the cavity (m)
β = Volumetric thermal expansion coefficient (1/K)
Δ = Difference
ε = Emissivity
λ = Thermal conductivity (W/(m-K))
$\lambda_{eq,h}$ = Equivalent thermal conductivity of the masonry in horizontal direction (W/(m-K))
$\lambda_{eq,v,d}$ = Equivalent thermal conductivity of the masonry in downward direction (W/(m-K))
$\lambda_{eq,v,u}$ = Equivalent thermal conductivity of the masonry in upward direction (W/(m-K))
ν = Kinematic viscosity (m^2/s)
ρ = Air density (kg/m^3)
ρ_r = Air density at reference temperature T_r (kg/m^3)
$\partial/\partial n$ = Derivative in the direction of external normal to the boundary

Acknowledgment

This article has been supported by Research Project MSM 6840770005.

References

Ait-Taleb T, Abdelbaki A and Zrikem Z (2008) Numerical simulation of coupled heat transfers by conduction, natural convection and radiation in hollow structures heated from below or above. *International Journal of Thermal Sciences* 47: 378–387.

Al-Hazmy MM (2006) Analysis of coupled natural convection-conduction effects on the heat transport through hollow building blocks. *Energy and Buildings* 38: 515–521.

Boukendil M, Abdelbaki A and Zrikem Z (2009) Numerical simulation by the FVM of coupled heat transfers by conduction, natural convection and radiation in honeycomb's hollow bricks. *Building Simulation* 2: 263–272.

Branco F, Tadeu A and Simões N (2004) Heat conduction across double brick walls via BEM. *Building and Environment* 39: 51–58.

Calcagni B, Marsili F and Paroncini M (2005) Natural convective heat transfer in square enclosures heated from below. *Applied Thermal Engineering* 25: 2522–2531.

Corcione M (2003) Effects of thermal boundary conditions at the sidewalls upon natural convection in rectangular enclosures heated from below and cooled from above. *International Journal of Thermal Sciences* 42: 199–208.

CSI (2002) Measurement Report No. 849 – Determination of the Thermal Resistance of Masonry Segment from Porotherm 44 P+D bricks. Prague: CSI Inc.

del Coz Díaz JJ, García Nieto PJ, Suárez Sierra JL and Betegón Biempica C (2008) Nonlinear thermal optimization of external light concrete multi-holed brick walls by the finite element method. *International Journal of Heat and Mass Transfer* 51: 1530–1541.

dos Santos GH and Mendes N (2009) Heat, air and moisture transfer through hollow porous blocks. *International Journal of Heat and Mass Transfer* 52: 2390–2398.

EN 1745 (2002) *Masonry and Masonry Products – Methods for Determining Design Thermal Values*. Brussels: CEN.

EN ISO 8990 (1996) *Thermal Insulation – Determination of Steady-state Thermal Transmission Properties – Calibrated and Guarded Hot Box*. Brussels: CEN.

EN ISO 6946 (2007) *Building Components and Building Elements – Thermal Resistance and Thermal Transmittance – Calculation Method*. Brussels: CEN.

EN ISO 10211 (2007) *Thermal Bridges in Building Construction – Heat Flows and Surface Temperatures – Detailed Calculations*. Brussels: CEN.

Fusegi T and Hyun JM (1991) A numerical study of 3D natural convection in a cube: effects of the horizontal thermal boundary conditions. *Fluid Dynamics Research* 8: 221–230.

Hasnaoui M, Bilgen E and Vasseur P (1992) Natural convection heat transfer in rectangular cavities partially heated from below. *Journal of Thermophysics and Heat Transfer* 6: 255–264.

Laccarrière B, Lartigue B and Monchoux F (2003) Numerical study of heat transfer in a wall of vertically perforated bricks: influence of assembly method. *Energy and Buildings* 35: 229–237.

Li LP, Wu ZG, He YL, Lauriat G and Tao WQ (2008a) Optimization of the configuration of $290 \times 140 \times 90$ hollow bricks with 3-D numerical simulation by finite volume method. *Energy and Buildings* 40: 1790–1798.

Li LP, Wu ZG, He YL, Lauriat G and Tao WQ (2008b) Numerical thermal optimization of the configuration of multi-holed clay bricks used for constructing building walls by the finite volume method. *International Journal of Heat and Mass Transfer* 51: 3669–3682.

Lorente S, Petit M and Javelas R (1996) Simplified analytical model for thermal transfer in vertical hollow brick. *Energy and Buildings* 24: 95–103.

Mentor Graphics (2008) FloVENT 8.1. Wilsonville, Oregon.

Sidik NAC (2009) Prediction of natural convection in a square cavity with partially heated from below and symmetrical cooling from sides by the finite difference lattice Boltzmann method. *European Journal of Scientific Research* 35: 347–354.

Sun J and Fang L (2009) Numerical simulation of concrete hollow bricks by the finite volume method. *International Journal of Heat and Mass Transfer* 52: 5598–5607.

Vasile C, Lorente S and Perrin B (1998) Study of convective phenomena inside cavities coupled with heat and mass transfer through porous media – application to vertical hollow bricks – a first approach. *Energy and Buildings* 28: 229–235.

Wakashima S and Saitoh TS (2004) Benchmark solutions for natural convection in a cubic cavity using the high-order time-space method. *International Journal of Heat and Mass Transfer* 47: 853–864.